Research on Chemical Intermediates (2021) 47:303–324
https://doi.org/10.1007/s11164-020-04333-2

Ambient base-free glycerol oxidation over bimetallic PdFe/SiO_2 by in situ generated active oxygen species

Ricci Underhill[1] · Mark Douthwaite[1] · Richard J. Lewis[1] · Peter J. Miedziak[1,2] · Robert D. Armstrong[1] · David J. Morgan[1] · Simon J. Freakley[1,3] · Thomas Davies[1] · Andrea Folli[1] · Damien M. Murphy[1] · Qian He[1,4] · Ouardia Akdim[1] · Jennifer K. Edwards[1] · Graham J. Hutchings[1]

Received: 17 October 2020 / Accepted: 26 October 2020 / Published online: 5 January 2021

Abstract

Low temperature oxidation of alcohols over heterogeneous catalysts is exceptionally challenging, particularly under neutral conditions. Herein, we report on an efficient, base-free method to oxidise glycerol over a 0.5%Pd-0.5%Fe/SiO_2 catalyst at ambient temperature in the presence of gaseous H_2 and O_2. The exceptional catalytic performance was attributed to the in situ formation of highly reactive surface-bound oxygenated species, which promote the dehydrogenation on the alcohol. The PdFe bimetallic catalyst was determined to be significantly more active than corresponding monometallic analogues, highlighting the important role both metals have in this oxidative transformation. Fe leaching was confirmed to occur over the course of the reaction but sequestering experiments, involving the addition of bare carbon to the reactions, confirmed that the reaction was predominantly heterogeneous in nature. Investigations with electron paramagnetic resonance spectroscopy suggested that the reactivity in the early stages was mediated by surface-bound reactive oxygen species; no homogeneous radical species were observed in solution. This theory was further evidenced by a direct H_2O_2 synthesis study, which confirmed that the presence of Fe in the bimetallic catalyst neither improved the synthesis of H_2O_2 nor promoted its decomposition over the PdFe/SiO_2 catalyst.

✉ Mark Douthwaite
douthwaitejm@cardiff.ac.uk

✉ Graham J. Hutchings
hutch@cardiff.ac.uk

[1] Cardiff Catalysis Institute, School of Chemistry, Cardiff University, Main Building, Park Place, Cardiff CF10 3AT, UK

[2] School of Applied Sciences, University of South Wales, Pontypridd CF37 4AT, UK

[3] Department of Chemistry, University of Bath, Claverton Down, Bath BA2 2AY, UK

[4] Department of Materials Science and Engineering, Faculty of Engineering, National University of Singapore, Singapore, Singapore

Keywords Glycerol · Oxidation · In situ · Ambient · PdFe

Introduction

Demand for bio-derived liquid fuel production is projected to increase steadily over the coming years. This is due to a global drive towards decoupling economic growth from fossil fuels and a shift towards renewable, sustainable fuels [1]. Current technologies for the extraction and refining of fossil fuels are comparably efficient and economical. As such, further process development is required in order to reduce the economic deficit separating the fossil fuel and bio-derived fuel industries.

A number of processes for producing bio-derived liquid fuels are currently operated commercially.[1] Of these, the production of biodiesel through transesterification of vegetable fats is perhaps the most promising [2, 3]. However, the product stream for this process contains approximately 10 wt% yield of glycerol, which is considered a low-value waste by-product. One possible way to offset the economic deficit between bio- and fossil fuels would be the development of efficient technologies for valorising this waste glycerol.

Catalytic upgrading of glycerol is not a novel concept [4, 5]. Indeed, aerobic oxidation of glycerol over noble metal catalysts is well documented [6, 7]. The highly functionalised nature of glycerol means that it lends itself well as a model substrate for studying how physicochemical properties of catalysts drive selectivity in the oxidation of alcohols and carbonyl species. This is compounded with the numerous products that form during glycerol oxidation, many of which are of commercial interest. The reaction conditions and catalyst used can dramatically influence the product selectivity, lactic acid [8, 9], dihydroxyacetone [10] and glyceric acid [11] have all been targeted as products for this reaction.

For liquid phase alcohol oxidation, it is widely accepted that the rate determining step is the C-H bond activation in the alcohol dehydrogenation [9], although to the best of our knowledge, this has yet to be confirmed experimentally using glycerol as a substrate. It is, however, evidenced indirectly as the application of stoichiometric base, such as NaOH, dramatically enhances the rate of reaction [7, 12]. DFT calculations for ethanol oxidation over Au nanoparticles reveal that Au-hydroxide species assist with alcohol deprotonation and dramatically reduced the activation barrier for the subsequent C-H bond activation [13, 14]. Various studies have postulated that the presence of hydroxide allows for an additional C-H bond activation pathway, in addition to beta-hydride elimination, through H-abstraction [15, 16]. This is, therefore, likely to be why such significant rate enhancements are observed for alcohol oxidation in the presence of base.

Despite progress in this area, reaction rates remain substantially lower under base-free conditions. For this reason, alternative strategies must be considered, if the oxidation of glycerol under ambient temperature and base-free conditions is to be realised on a commercial scale. While O_2 utilisation is desirable, use of a more reactive oxidising agent might prove to be an effective way to promote alcohol oxidation reactions under base-free conditions. An example of such an oxidant being hydrogen peroxide (H_2O_2).

H_2O_2 is an environmentally benign oxidant with the sole by-product of its decomposition being water. This contrasts with common oxidants such as perchlorates, permanganates and chromate-based reagents, which often produce unwanted, hazardous by-products. These incur a significant economic cost, due to downstream separation of waste streams. Commercial H_2O_2 synthesis via the anthraquinone oxidation process requires constant replacement of the anthraquinone carrier, due to unselective and irreversible hydrogenation of the carrier molecule. Therefore, H_2O_2 production is only economical on a relatively large scale, requiring that H_2O_2 be stored or transported at high concentrations, typically in excess of 70 wt%, in the presence of acid stabilising agents, prior to dilution at point of use. Due to hazardous nature of highly concentrated H_2O_2 solutions, this has significant technological and economic impacts [17]. A preferable alternative towards on-site, small scale H_2O_2 production would be the direct synthesis from molecular H_2 and O_2 [18].

Many studies have reported utilisation of preformed H_2O_2 as oxidant for glycerol oxidation. These studies have focussed on a range of different catalysts, including various supported metal catalysts [19–25] and metal oxides [26–34]. McMorn et al. [35] assessed metal-doped silicate (containing Ti, V or Fe) and aluminophosphate catalysts (containing Cr, V, Mn or Co) for oxidation of glycerol with H_2O_2, reporting low yields of the desired partial oxidation products. Subsequently, double-layered hydroxide (DLH)-supported transition metal complexes were reported as active for glycerol oxidation under comparable reaction conditions [10]. Indeed, a DLH-upported Cr(III) complex was reported to afford reasonable selectivity towards dihydroxyacetone (DHA) at high glycerol conversions (59.3% selectivity at 85.5% conversion). Additional investigations by Laurie et al. [36] and Farnetti et al. [37] attempted to propagate Fenton-type chemistry through combining Fe salts with H_2O_2. In both cases, relatively high selectivity towards C_3 products was observed, underlining the potential of using Fe-based species in this reaction.

In this study, a highly active heterogeneous catalytic system is reported for the oxidation of glycerol under base-free conditions. A 1 wt% PdFe/SiO_2 catalyst is used to synthesise surface-bound active oxygen species directly from H_2 and O_2 in situ which subsequently assists with the catalytic oxidation of glycerol. To the best of our knowledge, despite the abundance of literature in this area, this is the first example of invoking this strategy for this popular catalytic transformation.

Experimental

Catalyst preparation

Catalysts were prepared using a modified impregnation procedure based on that previously reported in the literature [38]. For the typical preparation of a 1 wt%PdFe/SiO_2 catalyst (Fe:Pd–0.5:0.5 wt%), the requisite amount of $PdCl_2$ (Sigma-Aldrich, ≥ 99.999%) solution (6 mg/mL Pd, 0.58 M HCl) and $FeCl_3$.6 H_2O (Sigma-Aldrich, ≥ 99%) solution (6 mg/mL Fe) were added to a 50 mL round bottom flask. Deionised water was then added to achieve a total solution volume of 16 mL. The solution was then heated to 60 °C with 1000 rpm stirring, and the required amount

of SiO_2 (Fisher Scientific, 60 Å particle size) support was added to produce 2 g of supported metal catalyst over 8–10 min. After complete addition of the support, the mixture was heated to 95 °C with stirring (1000 rpm) for 16 h to allow complete evaporation of the water. The dried catalyst was then recovered and ground using a pestle and mortar. The ground catalyst was then treated under a flow of 5% H_2/Ar (BOC) at 500 °C for 4 h (10 °C min^{-1} ramp rate). The treated catalyst was then allowed to cool to room temperature under a flow of 5% H_2/Ar (BOC).

Two corresponding monometallic catalysts were also prepared using the procedure described above. For this, requisite quantities of $FeCl_3 \cdot 6H_2O$ and $PdCl_2$ were used for the synthesis of 0.5wt%Fe/SiO_2 and 0.5 wt%Pd/SiO_2 catalysts, respectively.

Catalyst characterisation

HR-TEM (high-resolution transmission electron microscopy) and HAADF-STEM (high-angle annular dark field scanning transmission electron microscopy) analyses were performed in a JEOL JEM-2100 microscope at 200 kV. Energy dispersive X-ray spectroscopy (EDS) analysis was carried out using an Oxford Instruments X-Max^N analyser and Aztec software. Samples were supported onto holey carbon film copper grids.

Catalyst testing

Reaction procedure—in situ generated H_2O_2

Glycerol oxidation reactions were performed in a Parr stainless steel autoclave fitted with a PTFE liner and a nominal reactor volume of 50 mL. In a typical reaction, the PTFE liner was charged with an aqueous glycerol solution (10 mL, 0.3 M, Sigma-Aldrich, ≥ 99.5%) and catalyst (50 mg). The PTFE liner was then inserted into the reactor and the reactor sealed. The reactor was then purged three times with a dilute hydrogen mixture (5%H_2/CO_2, 100 psi). The reactor was then charged with 420 psi of 5% H_2/CO_2 and 160 psi of 25% O_2/CO_2, 160 psi to give a H_2: O_2 ratio of 1:2. The reactor was then heated to 30 °C and stirring commenced (1200 rpm) for 6 h unless otherwise stated. For recharge experiments, gases were vented and recharged at 1 h intervals. After the desired reaction time, the reactor was vented and solution collected. Following filtration, liquid products were quantified using high performance liquid chromatography (HPLC).

Reaction procedure—external addition of H_2O_2

Glycerol oxidation reactions were performed in a Parr stainless steel autoclave fitted with a PTFE liner and a nominal reactor volume of 50 mL. In a typical reaction, the PTFE liner was charged with an aqueous glycerol (Sigma-Aldrich, ≥ 99.5%) solution (10 mL, 0.3 M), catalyst (0.05 g) and hydrogen peroxide (50 wt% in H_2O stabilised,

Fluka, volume stated). The PTFE liner was then inserted into the reactor and reactor sealed. The reactor was then purged thrice with 25%O_2/CO_2 at 100 psi. The reactor was then charged with 580 psi of 25% O_2/CO_2. The reactor was then heated to 30 °C and stirring commenced (1200 rpm). After the desired reaction time, the reactor was vented and solution collected. Following filtration, liquid products were quantified using HPLC.

Reaction procedure—direct synthesis of H_2O_2 from molecular H_2 and O_2

Hydrogen peroxide synthesis was evaluated using a Parr Instruments stainless steel autoclave with a nominal volume of 100 mL and a maximum working pressure of 14 MPa. To test each catalyst for H_2O_2 synthesis, the autoclave was charged with catalyst (0.01 g), solvent (5.6 g MeOH and 2.9 g H_2O). The charged autoclave was then purged three times with 5% H_2/CO_2 (100 psi) before filling with 5% H_2/CO_2 to a pressure of 420 psi, followed by the addition of 25% O_2/CO_2 (160 psi). The temperature was then decreased to 2 °C followed by stirring (1200 rpm) of the reaction mixture for 0.5 h. The above reaction parameters represent the optimum conditions we have previously used for the synthesis of H_2O_2 [39]. H_2O_2 productivity was determined by titrating aliquots of the final solution after reaction with acidified $Ce(SO_4)_2$ (0.01 M) in the presence of ferroin indicator. Catalyst productivities are reported as mol $H_2O_2 kg_{cat}^{-1}$ h^{-1}.

Reaction procedure—degradation of H_2O_2

Catalytic activity towards H_2O_2 was determined in a manner similar to the direct synthesis activity of a catalyst. The autoclave was charged with MeOH (5.6 g), H_2O_2 (50 wt% 0.69 g) HPLC standard H_2O (2.21 g) with the solvent composition equivalent to a 4 wt% H_2O_2 solution. Prior to the addition of catalyst (0.01 g) from the solution two aliquots of 0.05 g was removed and titrated with acidified $Ce(SO_4)_2$ solution using ferroin as an indicator to determine an accurate concentration of H_2O_2 at the start of the reaction. The autoclave was pressurised with 420 psi 5% H_2/CO_2 and cooled to 2 °C, and the reaction mixture was stirred at 1200 rpm for 0.5 h. After the reaction was complete, the catalyst was removed from the reaction solvents and as previously two aliquots of 0.05 g were titrated against the acidified $Ce(SO_4)_2$ solution using ferroin as an indicator. The degradation activity is reported as mol $H_2O_2 kg_{cat}^{-1}$ h^{-1}. Note: The reaction conditions used within this study operate below the flammability limits of gaseous mixtures of H_2 and O_2.

Product analysis and catalyst evaluation

Both glycerol conversion and reaction products were quantified by HPLC using an Agilent 1260 Infinity series HPLC fitted with a MetaCarb 67 h column (column temp = 50 °C) and both RID and DAD detectors. 0.1% H_3PO_4 in deionised H_2O (Fisher Scientific, HPLC grade) was used as the mobile phase, and the flow rate was fixed at 0.8 mL min^{-1}. Calibrations were performed using known standards.

Nuclear magnetic resonance (NMR) was used for qualitative analysis of the radical trapping compounds. For this, ^1H NMR was performed at ambient temperatures on a 500 MHz Bruker Avance III HD spectrometer fitted with a Prodigy cryoprobe. Due to the strong solvent peak arising from H_2O, H_2O suppression was utilised. To the NMR tube was added filtered reaction solution (0.7 mL) and deuterium oxide (D_2O, 0.1 mL, Sigma-Aldrich). Additionally, a glass ampule containing 1 wt% TMS/$CDCl_3$ (Sigma-Aldrich) was added as internal standard.

The X-band (ca. 9.5 GHz) continuous wave (CW) EPR spectra were recorded on a Bruker EMX Micro spectrometer equipped with a Bruker ER4123-D dielectric resonator, operating at room temperature. Before each measurement, samples coming from the flow reactor where deoxygenated for 20 min under N_2 flow. Spectra were recorded at 298 K using the following instrumental conditions: $3.17 \cdot 10^3$ receiver gain; 100 kHz modulation frequency; 1.0 Gauss modulation amplitude and 3.282 mW microwave power. Experimental spectra were simulated using the EasySpin package [40] operating within the Mathworks MATLAB environment.

The concentration of leached metals in product streams was quantified through microwave plasma atomic emission spectroscopy (MP-AES) using an Agilent MP-AES 4100. Post-reaction solutions were filtered using PTFE syringe filters (0.45 μm) prior to analysis for Fe and Pd. Emission lines were calibrated using commercial standards (Sigma-Aldrich).

Results and discussion

We recently demonstrated the potential of using a 1 wt% Pd-Fe/SiO_2 catalyst towards phenol oxidation in wastewater streams [41]. The improved performance of this catalyst, compared to the well-studied AuPd analogue, was attributed to the formation and utilization of in situ formed H_2O_2 from H_2 and O_2. It was proposed that the material served as a multifunctional catalyst; the Pd component was proposed to be responsible for the generation of H_2O_2, while the Fe was responsible for the generation of the active oxygen species involved in the oxidation of phenol and its intermediates. Given the highly active nature of this catalyst, it was of profound interest to us to establish whether the catalyst, under similar base-free conditions, could be used for selective oxidation. The abundance of literature on glycerol oxidation, and the notion that it is exceptionally difficult to activate at low temperatures and neutral conditions, it represented an ideal substrate for these investigations.

The 1% PdFe/SiO_2 catalyst was synthesised via a modified impregnation methodology, described previously [38]. TEM was used to assess the size of the particles on the SiO_2 support (Fig. 1a and b). These experiments confirmed that the catalyst comprised a distribution of small bimetallic nanoparticles with mean particle size of approximately 3.2 nm (SD = 0.8). Further investigation by HAADF-STEM identified that some larger particles were also present in the catalyst. A representative 40 nm PdFe particle and corresponding EDXS is presented in Fig. 1c and d, respectively. In the larger particles, it is evident that Pd and Fe components are alloyed.

Given the conclusions from our previous work [41], it was important to establish how efficient this catalyst, and its monometallic counterparts were at catalysing the direct synthesis and subsequent degradation of H_2O_2. A series of experiments were therefore conducted to investigate this, the results of which can be found in Table 1. Interestingly, the presence of Fe in the catalyst had very little influence on the rate of H_2O_2 synthesis; the productivity of H_2O_2 was determined to be 69 and 66 mol $H_2O_2 kg_{cat}^{-1}$ h^{-1} for the 0.5% Pd/SiO_2 and 0.5%Pd-0.5%Fe/SiO_2 catalysts, respectively. The monometallic Fe catalyst unsurprisingly, exhibited no activity towards H_2O_2 synthesis. Similar findings were observed when H_2O_2 degradation was investigated over the three catalysts. The presence of Fe in the bimetallic catalyst did not meaningfully increase the rate of H_2O_2 degradation compared to the monometallic 0.5%Pd/SiO_2 analogue with degradation activity of 255 and 276

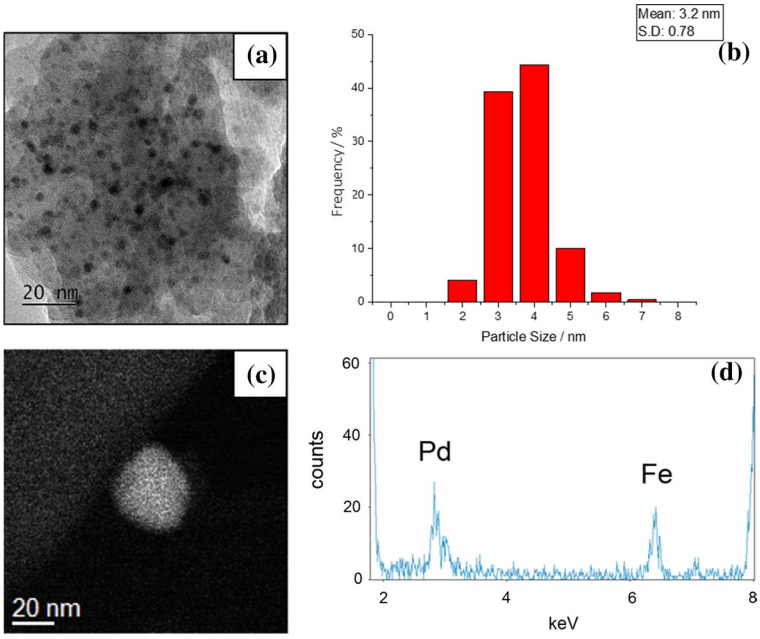

Fig. 1 Representative bright field transmission electron micrograph (**a**) and corresponding particle size distributions (**b**) of as prepared 0.5%Pd-0.5%Fe/SiO_2 catalyst prepared by a modified impregnation methodology (5%H_2/Ar, 500 °C, 4 h, ramp rate = 10 °C min^{-1}). HAADF-STEM image (**c**) and the corresponding X-ray energy dispersive spectrum (**d**) of a large 30–40 nm particle evidencing alloying of Pd and Fe

Table 1 Catalytic activity of SiO_2 supported monometallic and bimetallic catalysts towards H_2O_2 synthesis and its subsequent degradation

Catalyst	Productivity/mol $H_2O_2kg_{cat}^{-1}$ h^{-1} [a]	H_2O_2 Degradation/ mol $H_2O_2kg_{cat}^{-1}$ h^{-1} [b] (%)
0.5 wt%Pd/SiO_2	69	255 (6)
0.5 wt%Pd–0.5wt% Fe/SiO_2	66	276 (6)
0.5 wt% Fe/SiO_2	0	177 (4)

[a]H_2O_2 direct synthesis reaction conditions: Catalyst (0.01 g), H_2O (2.9 g), MeOH (5.6 g), 5% H_2/CO_2 (420 psi), 25% O_2/CO_2 (160 psi), 0.5 h, 2 °C 1200 rpm. [b]H_2O_2 degradation reaction conditions: Catalyst (0.01 g), H_2O_2 (50 wt% 0.68 g) H_2O (2.22 g), MeOH (5.6 g), 5% H_2/CO_2 (420 psi), 0.5 h, 2 °C 1200 rpm

mol $H_2O_2kg_{cat}^{-1}$ h^{-1} observed for these two catalysts, respectively. The monometallic 0.5%Fe/SiO_2 catalyst was however also found to catalyse H_2O_2 degradation, exhibiting an activity of 177 mol $H_2O_2kg_{cat}^{-1}$ h^{-1} for this competitive reaction. Given that the sum of H_2O_2 degradation activity over the two monometallic catalysts is greater than that observed over the corresponding bimetallic catalyst, it appears as though the presence of Fe is able to inhibit the formation of water, with recent studies reporting the ability of a range of secondary transition metals to similarly improve catalytic performance towards H_2O, with the modulation of Pd oxidation state and inhibition of contiguous Pd ensembles typically attributed as the cause for enhanced catalytic selectivity [42–44].

The performance of the bimetallic 0.5%Pd-0.5%Fe/SiO_2 catalyst was subsequently assessed for base-free glycerol oxidation, in the presence of H_2 and O_2. The results from this experiment are displayed in Fig. 2a. Glycerol conversion was

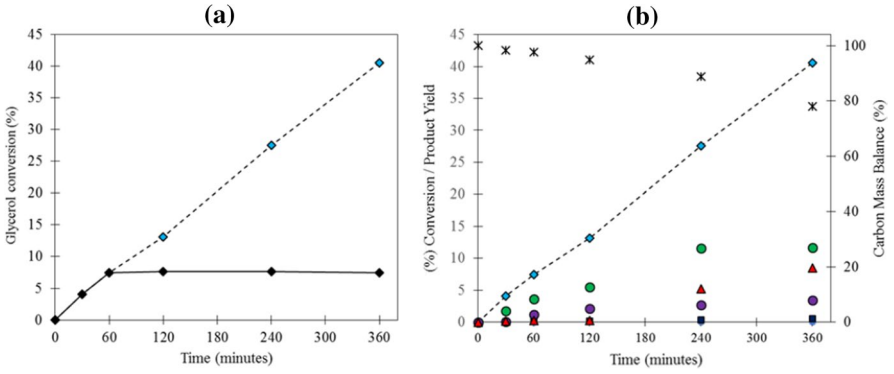

Fig. 2 Glycerol oxidation over a 0.5wt.%Pd-0.5wt.%Fe/SiO_2 with H_2O_2 generated in situ. **a** The effect of introducing hourly of H_2 / O_2 recharging cycles. **b** Glycerol conversion, product yields and carbon mass balance over a 6 h reaction with hourly recharging of H_2 and O_2. Reaction Conditions: 10 g 0.3 M glycerol solution, 420 psi 5%H_2 / CO_2, 160 psi 25%O_2 / CO_2, 50 mg 0.5wt.%Pd-0.5wt.%Fe / SiO_2, 1200 rpm stirring, 30 °C . Black diamond glycerol conversion with no gas recharges Blue diamond glycerol conversion with hourly gas replacement. Green circle glyceraldehyde, Violet circle dihydroxyacetone, Red triangle formic acid, Black square oxalic acid, Blue diamond glycolic acid. Asterisk carbon mass balance. (Color figure online)

determined to be linear with time for the initial 1 h of reaction, after which no further glycerol conversion was observed (up to 6 h on-line). Given that active oxygen species are considered to be the oxidant in this reaction, the rate at which both glycerol and partial oxidation products (GLD, DHA etc.) are converted, is limited by the rate in which these species are formed. Furthermore, the stoichiometric excess of O_2 to H_2 in the reactant gas could indicate that the lack of catalytic turnover at times greater than 1 h, is evidence of a H_2 limitation. Indeed, this proposal is further strengthened by the fact that O_2 is more soluble in the reaction solvent (H_2O) than H_2 [45, 46]. To determine whether this was the case, an additional experiment was conducted, whereby the reactor was de-pressurised and replenished with reactant gases every hour for 6 h. The rate of glycerol conversion under these conditions is also shown in Fig. 2a. When H_2 and O_2 were regularly replenished, the glycerol conversion continued to increase linearly after the first hour of reaction, confirming that in the absence of gas replenishment, the reaction is indeed likely to be limited by the availability of H_2.

The product distribution when replenishment cycles were applied is displayed in Fig. 2b. The data indicate that both the primary and secondary alcohols can undergo oxidative dehydrogenation to produce either glyceraldehyde (GLD) or DHA, respectively. Increased yields of GLD are observed, suggesting that the activation of the primary alcohol is more favourable than that of the secondary alcohol. It should be noted, that increased quantities of formic acid (FA) are also observed with time. This is unsurprising, given that FA is considered to be one of the terminal oxidation products in this reaction.[6,30] It is, however, unusual that comparable quantities of C_2 products are not also observed, suggesting that a direct route for the conversion of GLD or DHA to FA may exist. Alternately, it is possible that additional unidentified compounds are formed under reaction conditions. The observed decrease in carbon mass balance (CMB) with time is consistent with formation of other products, which might include the total oxidation product CO_2. Indeed, CO_2 has previously been reported as a product of aerobic glycerol oxidation [47]. Given that FA is known to readily decompose to CO, CO_2 and H_2 over supported Pd nanoparticles [48], it is likely some of the missing carbon represented in observed is present as either gaseous of CO or CO_2. However, the use of CO_2 as a diluent gas for both H_2 and O_2 reactant gases precludes us from determining if this is the case.

To gain a greater understanding of the mechanistic routes which lead to low CMBs, additional 6 h reactions (with gas replenishment) were conducted using DHA and GLD as substrates. Results of these experiments are displayed in Table 2 and highlight that there are clear differences in rates of carbon loss when different starting substrate is utilized. Over a 6 h period, 9.8% and 23.2% of the total carbon were unaccounted for with GLD and DHA oxidation, respectively. Interestingly, no apparent isomerisation between GLD and DHA was observed in either reaction. Given that this isomerisation is not observed, it suggests that both dehydrogenation of the primary and secondary alcohol in glycerol can occur. It also suggests that the unidentified reaction products can arise from both intermediates, but that the rate of the unknown pathway arising from DHA is faster. A study by McMorn et al. [35] illustrated that acetyls and esters can be formed when glycerol is oxidised with H_2O_2

Table 2 The oxidation of glycerol (0.3 M), glyceraldehyde (0.23 M) and dihydroxyacetone (0.13 M) over a 0.5Pd-0.5%Fe/SiO_2 under different gas compositions

Substrate	Reactant gases	χ Glycerol /%	Product yields/%							CMB (%)
			GLD	DHA	GLA	GLYOX	GLO	FA	OXA	
Glycerol	H_2+O_2	40.6	14.6	4.2	0.0	0.0	0.7	3.5	0.1	82.6
	O_2	0.5	0.0	0.1	0.0	0.0	0.0	0.0	0.0	99.6
GLD	H_2+O_2	*40.8*	0.0	0.0	10.0	2.4	4.9	14.0	0.7	91.2
	O_2	*0*	–	–	–	–	–	–	–	–
DHA	H_2+O_2	31.8	0.0	0.0	0.0	0.8	7.3	0.0	0.5	76.8
	O_2	0	–	–	–	–	–	–	–	–

Reaction conditions: 10 g 0.3 M glycerol solution, 420 psi 5%H_2/CO_2, 160 psi 25%O_2/CO_2, 50 mg 0.5 wt%Pd-0.5 wt%Fe / SiO_2, 6 h, 1200 rpm stirring, 30 °C. GLY (glycerol), GLD (glyceraldehyde), DHA (dihydroxyacetone), GLYOX (glyoxylic acid), GLO (glycolic acid), GLA (glyceric acid), FA (formic acid), OXA (oxalic acid), CMB (carbon mass balance), χ (conversion)

under base-free conditions. A reaction scheme for glycerol oxidation the products observed is proposed in Scheme 1.

It is proposed that two GLD molecules can partake in an acid-promoted condensation reaction to form acetyl species. This is likely given the mildly acidic reaction medium; a consequence of CO_2, which serves as a diluent for O_2 and H_2, dissolution in the aqueous medium [49]. In competition with this pathway, it is proposed that GLD can either undergo a sequential oxidation to GLA or undergo a C–C scission to from GLO and FA. GLO can subsequently undergo subsequent oxidative transformation to glyoxylic acid (GLYOX) and oxalic acid (OXA). These reaction pathways are well established in the literature [7]; DHA can also undergo C–C scission reactions in a similar manor to produce GLO, GLYOX, OXA and FA. Interestingly however, FA was not observed as a product in DHA conversion. As discussed previously, FA can decompose to CO_2 and H_2, however given its complete absence in the product distribution; it's more likely that it is consumed in an esterification reaction with DHA; the product of which was observed in the previous study by McMorn et al. [35]

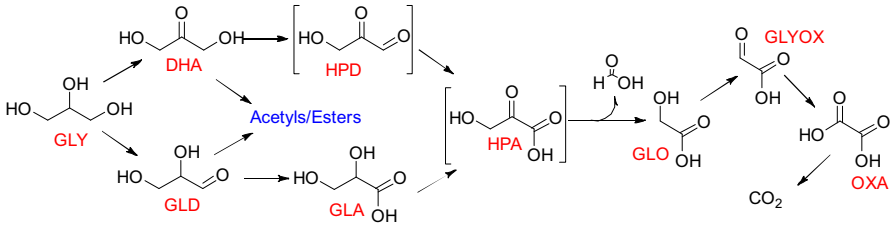

Scheme 1 Proposed schematic diagram for the oxidation of glycerol over the 0.5%Pd-0.5%Fe/SiO_2 catalyst. Abbreviations: GLY (glycerol), DHA (dihydroxyacetone), GLD (Glyceraldehyde), HPD (hydroxypyruvaldehyde), GLA (glyceric acid), HPA (hydroxy pyruvic acid), GLO (glycolic acid), GLYOX (glyoxylic acid), OXA (oxalic acid)

The aerobic oxidation of glycerol over Pd-supported catalysts has been reported [15]. To establish whether the observed glycerol conversion in Fig. 2a was a result of aerobic oxidation, an additional experiment was performed in the absence of hydrogen. The results from this experiment are displayed in Table 2 and Fig. 3a and confirm that no glycerol is converted in the absence of H_2. Additional studies were also conducted under aerobic conditions utilizing GLD and DHA (also displayed in Table 2), and similarly low conversion was observed.

To investigate the role of each supported metal present in the 0.5%Pd-0.5%Fe/SiO_2 catalyst, monometallic 0.5%Pd/SiO_2 and 0.5%Fe/SiO_2 catalysts were also synthesised and tested for the oxidation of glycerol under the same reaction conditions. The results from these experiments are displayed in Fig. 3b. Both monometallic catalysts exhibit a far lower glycerol conversion; the 0.5%Pd/SiO_2 was however notably more active than the 0.5Fe/SiO_2 catalyst. Indeed, the sum of glycerol conversion over the two catalysts, which is representative of the same quantity of Pd and Fe present in the reaction of the bimetallic catalyst, is still notably lower, indicative of synergy between the Pd and Fe in the bimetallic catalyst.

As discussed previously, a number of studies have investigated the potential of using H_2O_2 as the oxidant for this reaction [10, 35]. These studies, however, used pre-synthesised H_2O_2, likely containing acidic stabilising agents, introduced at the start of the reaction. In order to compare how the addition of commercial H_2O_2 to the reaction in this way affected the glycerol conversion under our reaction conditions, additional experiments were conducted (Table 3). To ensure that the observed reactivity in the ex situ experiments was not limited by available H_2O_2, a stoichiometric excess of H_2O_2 was used (1.25: 1—mol H_2O_2: $mol_{glycerol}$). Over a 6 h reaction, the observed glycerol conversion rates were far lower when H_2O_2 was added as a reagent, regardless whether the reaction was run in an oxidative or reductive environment. The slight increase in performance under a reductive atmosphere may

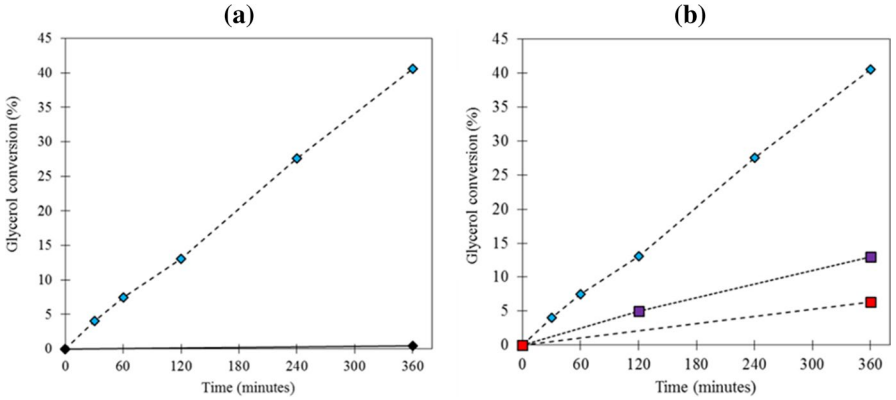

Fig. 3 **a** The effect of gas composition on glycerol conversion rates. Blue diamond 5%H_2/CO_2 with 25%O_2/CO_2 versus Black square 25%O_2/CO_2. **b** Glycerol conversion over 0.5 wt.% Pd/SiO_2 Violet square, 0.5 wt.% Fe/SiO_2 Red square and 0.5 wt.%Pd-0.5 wt.%Fe/SiO_2 Blue diamond catalysts with H_2O_2 generated in situ. Reaction Conditions: 10 g 0.3 M glycerol solution, 420 psi 5%H_2 / CO_2, 160 psi 25%O_2 / CO_2, 50 mg of catalyst, 1200 rpm stirring, 30 °C. (Color figure online)

Table 3 Comparison of in situ active oxygen species with *ex situ* addition of H_2O_2

Oxidant	Time/h	χ Glycerol /%	Product yields/%							CMB /%
			GLD	DHA	GLA	GLYOX	GLO	FA	OXA	
H_2+O_2	1	7.5	3.7	2.4	0.0	0.0	0.2	0.6	< 0.1	99.3
H_2+O_2	6	40.6	14.6	4.2	0.0	0.0	0.7	3.5	0.1	82.6
$O_2+4\%H_2O_2$	6	7.8	2.5	0.5	0.4	0.0	0.8	4.8	0.0	101.1
$H_2+4\%H_2O_2$	6	13.5	5.5	1.1	0.3	0.0	0.6	2.6	0.0	96.8

Reaction conditions: 10 g 0.3 M glycerol solution, 420 psi $5\%H_2/CO_2$, 160 psi $25\%O_2/CO_2$ (or 580 psi $25\%O_2/CO_2$ for test with addition of H_2O_2), 50 mg 0.5%Pd-0.5%Fe/SiO_2, 1200 rpm stirring, 30 °C. GLD (glyceraldehyde), DHA (dihydroxyacetone), GLYOX (glyoxylic acid), GLO (glycolic acid), GLA (glyceric acid), FA (formic acid), OXA (oxalic acid), CMB (carbon mass balance), χ (conversion)

be attributed to the H_2 promotion of the Fenton reaction, likely to be facilitated by the presence of leached Fe in solution [50] (Fig. 4). Nevertheless, these experiments clearly indicate that the oxidation of glycerol is far more efficient, when reactions are conducted in the presence of H_2 and O_2. Even if all the added H_2O_2 is utilized rapidly, given the stoichiometric excess used, the selectivity for its utilization in this reaction is likely to be very poor in comparison with the in situ approach. This data clearly illustrate that the activity of the 0.5%Pd-0.5%Fe/SiO_2 catalyst is likely governed by the formation of active surface species from H_2 and O_2 and not from the synthesis and consumption of H_2O_2, as originally suspected.

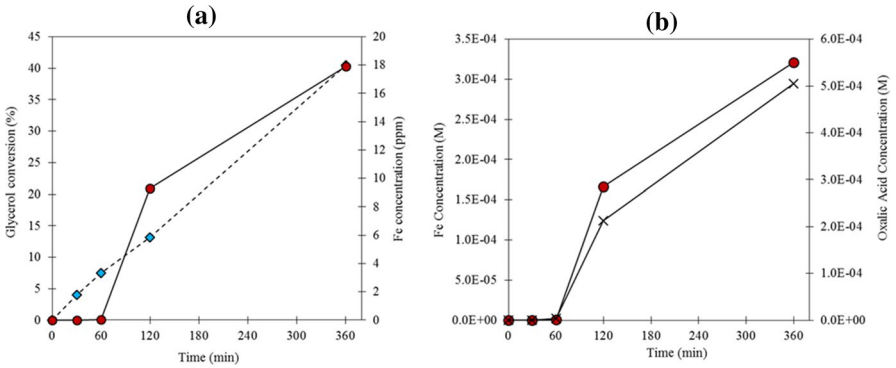

Fig. 4 **a** Glycerol conversion Blue diamond and Fe leaching (ppm) Red circle as a function of reaction time. **b** The concentration of leached Fe (M) Red circle and OXA concentration (M) as a function of time. Reaction Conditions: 10 g 0.3 M glycerol solution, 420 psi $5\%H_2$ / CO_2, 160 psi $25\%O_2$ / CO_2, 50 mg 0.5 wt.%Pd-0.5 wt.%Fe / SiO_2, 1200 rpm stirring, 30 °C. (Color figure online)

Comparing the effect of homogeneous versus heterogeneous Fe on catalytic performance

When employing heterogeneous catalysts in an aqueous medium, leaching of the active metals from the support can be problematic, especially when organic acids are present in the reaction mixture. To investigate whether any leaching of Fe and/or Pd occurred in these reactions, post reaction solutions were analysed via MP-AES. As illustrated in Fig. 4, while no Pd leaching was detected, significant leaching of Fe was observed. Interestingly, although the degree of Fe leaching increased with time, the rate of glycerol conversion remained unaffected. Homogeneous Fe species have been shown to be effective catalysts for oxidations with H_2O_2 [51]. It was therefore necessary to consider whether the contribution from Fe in this reaction was a result of hetero- or homogeneous catalysis.

A lack of Fe leaching during the initial 1 h of reaction indicates that leaching of Fe from the SiO_2 support is not the result of inherent instability of the metal-support interface. Indeed, no Fe leaching was observed when the catalyst was stirred in water for 6 h under reaction conditions. Fe leaching must therefore be due to supported metals interacting with reaction products. We have previously shown this to be the case for supported Fe catalysts in the degradation of phenol, with increased Fe leaching observed with increased concentrations of oxalic, acetic and formic acids [41]. Given that OXA can act as a powerful chelating agent, its concentration in the reaction solution was correlated with that of leached Fe. This data are illustrated in Fig. 4b. A strong correlation between these concentrations was observed, suggesting that the leaching of Fe into solution is likely to be primarily attributed to chelation by OXA. This is unsurprising, given that OXA is known to be an effective chelating agent; it has the ability to form both Fe^{2+} and Fe^{3+} oxalates in solution.

To determine whether the synergistic effect observed for 0.5%Fe-0.5%Pd/SiO_2 resulted from catalytically active Fe species in solution, carbon was added to sequester leached Fe from solution. A similar approach was successfully invoked by Armstrong et al. [52] to remove leached Pt from solution in the oxidation of glucose. The results from these experiments are displayed in Fig. 5. Addition of carbon (50 mg) at the beginning of the reaction led to a five-fold decrease in the Fe concentration in solution after 6 h, from 17.5 to 3.3 ppm. The addition of low quantities of carbon in this way had no significant effect upon glycerol conversion rates, indicating that the activity observed in this reaction is independent of leached Fe concentration. However, the addition of > 50 mg carbon led to decreased rates of glycerol conversion and effectively sequestered Fe from solution. In the presence of 200 mg of carbon, the glycerol conversion drops to *ca.* 25%. Given that only trace quantities of Fe were detected in the post reaction effluent in this reaction, we can confidently propose that the majority of glycerol is converted on the catalyst surface.

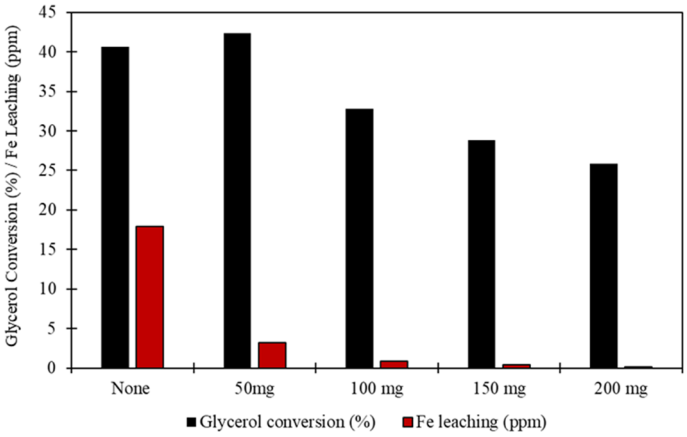

Fig. 5 The effect of adding an increasing mass of Norit SX1G carbon at $t=0$ upon glycerol conversion and leached Fe concentration. Reaction Conditions: 10 g 0.3 M glycerol solution, 420 psi 5%H_2/CO_2, 160 psi 25%O_2/CO_2, 50 mg 0.5 wt%Pd-0.5% wt.Fe/SiO_2, X mg Norit SX1G, 6 h, 1200 rpm stirring, 30 °C. Gases were vented and recharged hourly

Investigating the nature of the oxidising species

It is clear that 0.5%Fe-0.5%Pd/SiO_2 catalyst effectively catalyses the oxidation of glycerol under mild reaction conditions using oxidising species generated catalytically in situ from H_2 and O_2. The nature of the oxidising species, however, remains elusive. Given the reactivity of the chemical components, it is possible that some contribution to the observed activity may be attributed to two sequential catalytic processes; (i) direct, Pd-catalysed H_2O_2 synthesis from H_2 and O_2 and (ii) Pd/Fe-catalysed H_2O_2 conversion to yield oxidising hydroxyl (HO·) and/or hydroperoxy (HOO·) radicals in solution. An alternative mechanism for oxidation could involve interaction between the substrate and surface-bound reactive oxygen species formed from H_2 and O_2. A number of studies have proposed mechanisms whereby Pd sites catalyse H_2O_2 formation via a surface-bound *OOH intermediate [53, 54]. While it is possible that such a mechanism is occurring in the reactions discussed, herein the relatively low rates of conversion observed over 0.5%Pd/SiO_2 when compared with 0.5%Fe-0.5%Pd/SiO_2 suggests that free radicals play a role in glycerol oxidation. To determine whether glycerol conversion is mediated by oxygen-based free radicals in solution, the radical trap 5,5-dimethyl-1-pyrroline *N*-oxide (DMPO) was added at the start of the reaction, and resulting product streams were analysed by EPR.

Control experiments in the absence of a catalyst but containing DMPO, glycerol and the H_2/O_2 gas charge, yielded an EPR spectrum which is consistent with formation of the DMPO-OH adduct (Fig. 6a). Under these conditions, no apparent glycerol conversion was observed. Addition of 0.5%Fe-0.5%Pd/SiO_2 to this reaction led to total loss of the DMPO-OH feature (Fig. 6b), suggesting that the catalyst is effectively terminating ·OH species. This was confirmed through addition of catalyst, but not glycerol to the reaction, with the resulting EPR spectrum showing no apparent DMPO-OH adduct formation (Fig. 6c). This appears

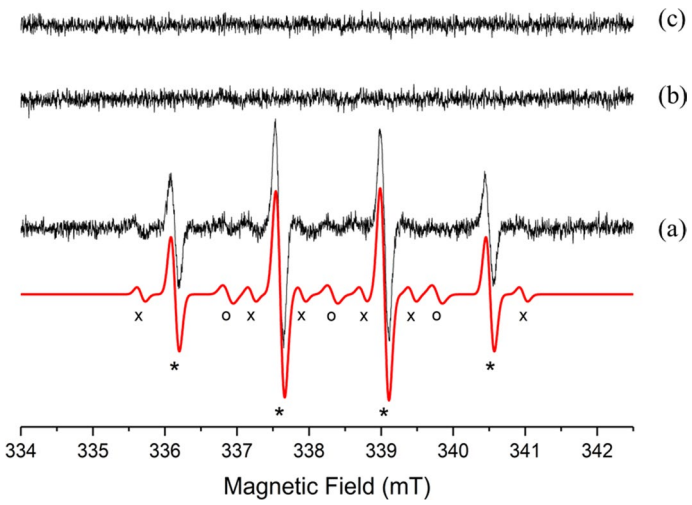

Fig. 6 X-band CW-EPR spectra (black traces) recorded at 298 K for **a** 5% H_2/CO_2 and 25%O_2/CO_2 in water in the presence of DMPO and absence of the catalyst; **b** 5% H_2/CO_2 and 25%O_2/CO_2 in water in the presence of DMPO and 50 mg of 0.5 wt%Pd-0.5 wt%Fe/SiO_2; **c** 5% H_2/CO_2 and 25%O_2/CO_2 in a 0.3 M aqueous solution of glycerol in the presence of DMPO and 50 mg of 0.5 wt%Pd-0.5 wt%Fe/SiO_2. EPR simulations are shown in red. The 1:2:2:1 signals marked with an asterisk, *, are indicative of the presence of DMPO-OH adduct: $g_{iso} = 2.0057 \pm 0.001$; $a_{iso}(^{14}N) = 41.62 \pm 0.95$ MHz; $a_{iso}(^{1}H) = 42.57 \pm 0.95$ MHz. The 1:1:1:1:1:1 signals marked with an **x** are indicative of the presence of a DMPO adduct generated by trapping a C-based radicals (most likely present as an impurity): $g_{iso} = 2.0057 \pm 0.001$; $a_{iso}(^{14}N) = 44.34 \pm 0.95$ MHz; $a_{iso}(^{1}H) = 64.01 \pm 0.95$ MHz. Finally, the 1:1:1 signals marked with an **o** are due to DMPO decomposition products, often present when DMPO spin trapping experiments are performed: $g_{iso} = 2.0057 \pm 0.001$; $a_{iso}(^{14}N) = 41.76 \pm 0.95$ MHz *Prior to EPR measurements, the reagents and catalyst were stirred together in an autoclave under reaction conditions for 5 min

counterintuitive, given that significant glycerol conversion is observed under these conditions. To rule out potential oxidative decomposition of the DMPO spin trap, quantitative ^{1}H NMR spectra were collected for the same solutions, with resonances normalised to an internal TMS standard at $\delta\ ^{1}H = 0.0$ ppm. It is clear from spectra in Fig. 7 and integrated peak areas in Table 4 that no significant DMPO conversion occurs during the 5 min reaction period. Formation of a DMPO-OH adduct would be expected to result in a downfield shift of resonance (d) and would lead to a change in the ratio of b, c, d: a. This was not observed, though appearance of an unknown species ($\delta\ ^{1}H = 2.43$ ppm) correlates with addition of 0.5%Fe-0.5%Pd/SiO_2 to the reaction (Figs. 6iii and 6iv). Given that the EPR/NMR experiments suggest a lack of DMPO-OH adduct formation in the catalysed reaction (Figs. 5b and 6iv), it is unlikely that glycerol oxidation is mediated by oxygen- based free radicals in solution. Rather, these data suggest formation of reactive surface-bound oxygen species and that it is through interaction with these that glycerol undergoes partial oxidation.

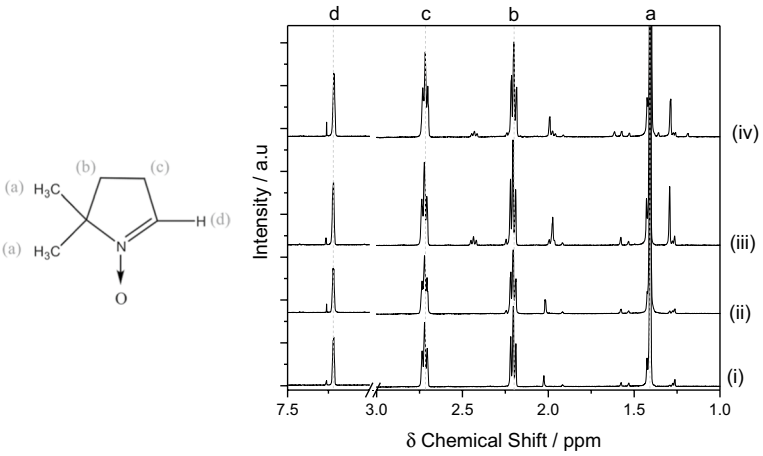

Fig. 7 ^{1}H NMR spectra of spin trap product solutions, inc. nmr assignment for DMPO. **i** 10 µL DMPO in 10 ml H_2O, **ii** 10 µL DMPO in 10 ml H_2O after 5 min reaction with H_2 and O_2, **iii** 10 µL DMPO in 10 ml H_2O after 5 min reaction with H_2, O_2 and 0.5 wt%Pd-0.5 wt%Fe/SiO_2, **iv** 10 µL DMPO in 10 ml 0.3 M glycerol solution after 5 min reaction with 5% H_2/CO_2, 25%O_2/CO_2 and 0.5 wt%Pd-0.5 wt%Fe/SiO_2

Discussion

The experimental results presented herein, particularly from the EPR experiments, are somewhat surprising and indicate that the observed reactivity does not stem from the formation of ·OH in situ. The data presented in Fig. 3 confirm that H_2 is required in the medium to convert glycerol under these conditions, thus, any contribution from an aerobic oxidation pathway, at least in a traditional sense, can be dismissed. As discussed previously, the RDS in this reaction is the alcohol dehydrogenation, deprotonation of the alcohol and subsequent activation of an adjacent C–H bond. The presence of an adjacent surface-bound hydroxy species on a model Au catalyst was proposed to dramatically reduce the activation barriers, for both these process [14]. The authors speculate, with evidence from DFT calculations, that this reduction in activation energy is attributable to the formation of superoxide (*OOH) and hydroxide (*OH) surface intermediates. It is therefore plausible to suggest that these intermediates are also responsible for the activity we observe over the 0.5%Pd-0.5%Fe/SiO_2 catalyst in the presence of H_2 and O_2.

The reduction of O_2 by H_2O, which leads to the formation of these intermediates, is likely to be rather energy intensive, which could explain why in the absence of base such poor activity is observed over heterogeneous catalysts. One can however envisage that O_2 reduction by dissociatively adsorbed hydrogen would be far more favourable; this is considered to be a key step in the direct synthesis of H_2O_2 which is commonly practiced at temperatures as low as 2 °C [55]. Based on this fact and through reference to previous work [14, 54], we can propose a mechanism for these transformations (Scheme 2) and highlight the importance of simultaneous oxygen reduction reactions. First, dissociative adsorption of H_2 occurs on a Pd site (Scheme 2, step 1), which is followed by heterolytic H* oxidation (Scheme 2, step 2)

Table 4 Integrated DMPO peak areas for ^{1}H NMR resonance peaks in Fig. 7

Experiment	δ 1.41 ppm (a)	δ 2.20 ppm (b)	δ 2.72 ppm (c)	δ 7.22 ppm (d)
(i) 10 µL DMPO in 10 ml H_2O	7.5	2.2	2.2	1
(ii) 10 µL DMPO in 10 ml H_2O after 5 min reaction with H_2 and O_2 *	7.3	2.2	2.2	1
(iii) 10 µL DMPO in 10 ml H_2O after 5 min reaction with H_2, O_2 and 0.5 wt% Pd-0.5 wt% Fe/SiO_2 *	7.3	2.2	2.2	1
(iv) 10 µL DMPO in 10 ml 0.3 M glycerol solution after 5 min reaction with H_2, O_2 and 0.5 wt% Pd-0.5 wt% Fe/SiO_2. *	7.2	2.2	2.2	1

Resonances integrated using TopSpin 3.5 NMR software and areas normalised to proton H^d at 7.22 ppm. Note: resonance at δ 1.41 overlaps with ^{1}H resonance of contaminant water present within the $CDCl_3$/TMS insert, hence deviation from the predicted 6:2:2:1 ratio (a:b:c:d). * 420 psi 5%H_2/CO_2, 160 psi 25%O_2/CO_2 Resonances integrated using TopSpin 3.5 NMR software and areas normalised to proton H^d at 7.22 ppm. Note: resonance at δ 1.41 overlaps with ^{1}H resonance of contaminant water present within the $CDCl_3$/TMS insert, hence deviation from the predicted 6:2:2:1 ratio (a:b:c:d). * 420 psi 5%H_2/CO_2, 160 psi 25%O_2/CO_2

Scheme 2 Proposed series of steps for glycerol (GLY) oxidation to glyceraldehyde (GLD) in the presence of H_2 and O_2. This example highlight the role of the *OOH intermediate in promoting proton abstractions from the alcohol moiety and adjacent α-carbon in the primary alcohol. Note: * corresponds to a surface active site

$$H_2 \rightleftharpoons 2H^* \quad (1)$$

$$H^* \rightleftharpoons H^+ + e^- + * \quad (2)$$

$$O_2 + ** \rightleftharpoons O_2** \quad (3)$$

$$H^+ + O_2** + e^- \rightleftharpoons OOH** \quad (4)$$

$$H^+ + OOH** + e^- \rightleftharpoons H_2O_2** \quad (5)$$

$$GLY* + 2OOH** \rightleftharpoons GLD + 2H_2O_2** \quad (6)$$

$$H_2O_2** \rightleftharpoons H_2O_2 + ** \quad (7)$$

and simultaneous adsorption of molecular oxygen (Scheme 2, step 3) sites. The proton formed from heterolytic oxidation of H* is subsequently transferred to molecular oxygen (O_2**) via proton–electron transfer (Scheme 2, step 4). This peroxide intermediate (HOO**) can then, either abstract a proton from the Pd in a subsequent proton–electron transfer to produce H_2O_2** (Scheme 2, step 5) or abstract a proton from either the alcohol moiety or from the α-carbon in an glycerol alkoxy intermediate also producing H_2O_2** (Scheme 2, step 6). H_2O_2** subsequently desorbs to liberate the two active sites (Scheme 2, step 7). We propose that these two processes are in direct composition, and their relative rates are dependent on surface coverage.

It is also important to consider the synergistic effect observed from introducing Fe into the Pd particles. McEwen and co-workers demonstrated that the deposition of Pd onto a Fe_2O_3 support could significantly enhance the reducibility of Fe^{3+} [56]. We therefore propose that in the 0.5%Pd-0.5%Fe/SiO_2 catalyst, the hydrogen formed from dissociative adsorption on Pd sites can spill over and reduce adjacent Fe_2O_3 to form Fe-OH/Fe-OOH species. We propose that this species also assist with deprotonation and activation of the C-H bond in the glycerol alkoxy adduct. This theory is further strengthened by the fact that an electrochemical study investigating alcohol oxidation over PdNi bimetallic catalysts concluded that the enhanced performance was attributed to the presence of *OOH species in the base metal component [57].

The preceding discussion provides an explanation into the activity observed from a heterogeneous perspective, but a small contribution from homogeneous Fenton chemistry cannot be excluded. This is most pertinent, especially given the ability of this catalyst to produce H_2O_2 directly from H_2O_2. In the reaction where almost all the Fe were successfully sequestered by carbon (Fig. 5), a notable drop in glycerol conversion was observed, glycerol conversion drops from 41% without carbon to 26% in the reaction with 200 mg of carbon. While the EPR experiments confirm that there is no suggestion of ·OH species in solution, these measurements were conducted at short reaction times (5 min), where the concentration of leached Fe is minimal (Fig. 4). We therefore speculate that the high catalytic performance observed over the 0.5%Pd-0.5%Fe/SiO_2 catalyst is attributable to both heterogeneous and homogeneous processes.

From the results acquired, it is difficult to assess how selective this catalyst is for glycerol oxidation. Fairly high concentrations of glyceraldehyde are produced, but experiments conducted using this as a substrate demonstrate that it is consumed under reaction conditions. Given the large quantities of formic acid it is plausible to

suggest that this catalyst reacts with many of the high value products of this reaction; only trace quantities of glyceric and tartronic acid are observed post reaction. Further work is required to explore whether there is opportunity to oxidise glycerol selectively using this methodology.

Conclusion

In conclusion, 0.5%Fe-0.5% Pd/SiO_2 prepared by a modified impregnation method is highly active for the base-free oxidation of glycerol at 30 °C. The reactivity of this catalyst is primarily attributed to the formation of active oxygen surface species; formed from the reduction of O_2 by dissociatively adsorbed hydrogen on Pd sites. The active oxygen species is proposed to be *OOH species, situated on both Fe and Pd sites. We speculate that some activity arises from homogeneous Fenton chemistry, despite the lack of evidence from EPR and NMR. Leaching of Fe species over the course of the reaction was observed, but sequestering experiments confirmed that the reaction was predominantly heterogeneous in nature. While this catalyst does not appear selective towards a given product, to the best of our knowledge, the observed rates of glycerol conversion are unparalleled, particularly under such a mild temperature and base-free condition. Future catalyst design studies might target improved reaction selectivity, while the system may also find application in the total catalytic oxidation of organic contaminants.

Memories of Michel Che

Michel was a great mentor to myself through since 1997 when I became Head of the School of Chemistry at Cardiff University. Michel had a connection with Cardiff through Damien Murphy who then had just been appointed to a lectureship. Previously Damien had worked with Michel and through this connection I got to know Michel.

Michel invited me as a visiting Professor to his University in Paris in June 2004. As I was still Head of School, I could only be in Paris part time and so I visited Paris early Monday until late Wednesday and was in Cardiff for the rest of the week. Michel was a perfect host. He would let me think about my science in the morning until about 11.30 and then we would walk together around Paris finding a wonderful restaurant for lunch and then arriving back at the lab at about 4 pm. This was a wonderful time as Michel was so knowledgeable and we had such wonderful walks around Paris. This time was important for me as I decided to concentrate more of my effort on gold catalysis, and Michel was an enthusiastic mentor in these efforts. I now look back to that time with Michel as a key point in my research career.

Michel played a leading part in the development of the Cardiff Catalysis Institute when we started in 2008. He served as the Chair of the external advisory board until January 2019 when I stepped down as the director and he then decided to withdraw from the board. His advice as chair was so important to us. He gave his time so freely to ensuring that others could succeed and we all appreciated this quality—he

just knew the right way to ensure progress could be made even when it was not apparent how this could be done at the start.

Michel loved Rugby Union and was a loyal French supporter. I was often able to get tickets to the Wales-France Six Nations matches when played in Cardiff. Michel would really enjoy these trips. Cardiff takes on a magical atmosphere on these match days and we had a great time. Sadly, in all the matches we enjoyed together we never once witnessed a French victory!

It goes without saying that Michel was a leading catalysis scientist, and this was recognised in the UK by the award of the 2009 RSC Centenary Prize. But, the most significant recognition in my opinion was the award of the RSC Faraday Lectureship and Prize in 2014. This is the oldest award of the RSC and is awarded only every two years. One of my fondest memories of Michel is having the opportunity to present him with the medal for this prize as I was President of the Faraday Division at the time (see the happy photo).

As I write this, I can hear his voice talking to me, reminding me of the walks we had, the rugby we watched and the science we discussed. We all miss him greatly.

Graham Hutchings.

Acknowledgements The authors wish to acknowledge the contribution of Selden Research Limited. We would also like to thank the Cardiff University TEM facility for the electron microscopy.

References

1. M. Balat, Policy **2**, 167 (2007)
2. A.F. Lee, J.A. Bennett, J.C. Manayil, K. Wilson, Chem Soc Rev **43**, 7887 (2014)
3. D.E. López, J.G. Goodwin, D.A. Bruce, J. Catal. **245**, 381 (2007)
4. P.S. Kong, M.K. Aroua, W.M.A.W. Daud, Renew. Sustain. Energy Rev. **63**, 533 (2016)
5. C.H. Zhou, J.N. Beltramini, G.Q. Lu, Chem. Soc. Rev. **37**, 527 (2008)
6. A. Villa, N. Dimitratos, C.E. Chan-Thaw, C. Hammond, L. Prati, G.J. Hutchings, Acc. Chem. Res. **48**, 1403 (2015)
7. B. Katryniok, H. Kimura, E. Skrzyńska, J.S. Girardon, P. Fongarland, M. Capron, R. Ducoulombier, N. Mimura, S. Paul, F. Dumeignil, Green Chem. **13**, 1960 (2011)
8. M. Douthwaite, N. Powell, A. Taylor, G. Ford, J.M. López, B. Solsona, N. Yang, O. Sanahuja-Parejo, Q. He, D.J. Morgan, T. Garcia, S.H. Taylor, ChemCatChem **12**, 3097 (2020)
9. R.K.P. Purushothaman, J. van Haveren, D.S. van Es, I. Melián-Cabrera, J.D. Meeldijk, H.J. Heeres, Appl. Catal. B Environ. **147**, 92 (2014)
10. X. Wang, C. Shang, G. Wu, X. Liu, H. Liu, Catalysts **6**, 101 (2016)
11. S. Carrettin, P. McMorn, P. Johnston, K. Griffin, G.J. Hutchings, Chem. Commun. **7**, 696 (2002)
12. J. Fu, Q. He, P.J. Miedziak, G.L. Brett, X. Huang, S. Pattisson, M. Douthwaite, G.J. Hutchings, Chem. A Eur. J. **24**, 2396 (2018)
13. M.S. Ide, R.J. Davis, Acc. Chem. Res. **47**, 825 (2014)
14. B.N. Zope, D.D. Hibbitts, M. Neurock, R.J. Davis, Science **330**, 74 (2010)

15. S. Carrettin, P. McMorn, P. Johnston, K. Griffin, C.J. Kiely, G.J. Hutchings, Phys. Chem. Chem. Phys. **5**, 1329 (2003)
16. M. Douthwaite, X. Huang, S. Iqbal, P.J. Miedziak, G.L. Brett, S.A. Kondrat, J.K. Edwards, M. Sankar, D.W. Knight, D. Bethell, G.J. Hutchings, Catal. Sci. Technol. **7**, 5284 (2017)
17. G. Centi, S. Perathoner, Catal. Today **143**, 145 (2009)
18. B. Puértolas, A.K. Hill, T. García, B. Solsona, L. Torrente-Murciano, Catal. Today **248**, 115 (2015)
19. E. Diguilio, E.D. Galarza, M.E. Domine, L.B. Pierella, M.S. Renzini, New J. Chem. **44**, 4363 (2020)
20. F. Zhang, X. Wang, G. Wu, C. Zhang, S. Song, J. Lan, ChemistrySelect **4**, 13876 (2019)
21. X. Wang, G. Wu, T. Jin, J. Xu, S. Song, Catalysts **8**, 505 (2018)
22. M.L. Faroppa, J.J. Musci, M.E. Chiosso, C.G. Caggiano, H.P. Bideberripe, J.L.G. Fierro, G.J. Siri, M.L. Casella, J. Catal. **37**, 1982 (2016)
23. M. Kapkowski, P. Bartczak, M. Korzec, R. Sitko, J. Szade, K. Balin, J. Lelątko, J. Polanski, J. Catal. **319**, 110 (2014)
24. C.A. Nunes, M.C. Guerreiro, J. Mol. Catal. A Chem. **370**, 145 (2013)
25. M. Ziolek, P. Decyk, I. Sobczak, M. Trejda, J. Florek, H.G.W. Klimas, A. Wojtaszek, Appl. Catal. A Gen. **391**, 194 (2011)
26. P. Chagas, M.A. Thibau, S. Breder, P.P. Souza, G.S. Caldeira, M.F. Portilho, C.S. Castro, L.C.A. Oliveira, Chem. Eng. J. **369**, 1102 (2019)
27. X. Wang, G. Wu, X. Zhang, D. Wang, J. Lan, J. Li, Catal. Letters **149**, 1046 (2019)
28. P.N. Amaniampong, Q.T. Trinh, J.J. Varghese, R. Behling, S. Valange, S.H. Mushrif, F. Jérôme, Green Chem. **20**, 2730 (2018)
29. S. Thanasilp, J.W. Schwank, V. Meeyoo, S. Pengpanich, M. Hunsom, Chem. Eng. J. **275**, 113 (2015)
30. B. Sarkar, C. Pendem, L.N. Konathala, R. Tiwari, T. Sasaki, R. Bal, Chem. Commun. **50**, 9707 (2014)
31. J. Souza, P.M.T.G. Souza, P.P. De Souza, D.L. Sangiorge, V.M.D. Pasa, L.C.A. Oliveira, Catal. Today **213**, 65 (2013)
32. M. Ziolek, I. Sobczak, P. Decyk, L. Wolski, Catal. Commun. **37**, 85 (2013)
33. J.P. Souza, T. Melo, M.A.L. De Oliveira, R.M. Paniago, P.P. De Souza, L.C.A. Oliveira, Appl. Catal. A Gen. **443–444**, 153 (2012)
34. L.C.A. Oliveira, M.F. Portilho, A.C. Silva, H.A. Taroco, P.P. Souza, Appl. Catal. B Environ. **117–118**, 29 (2012)
35. P. McMorn, G. Roberts, G.J. Hutchings, Catal. Lett. **63**, 193 (1999)
36. V.F. Laurie, A.L. Waterhouse, J. Agric. Food Chem. **54**, 4668 (2006)
37. E. Farnetti, C. Crotti, Catal. Commun. **84**, 1 (2016)
38. M. Sankar, Q. He, M. Morad, J. Pritchard, S.J. Freakley, J.K. Edwards, S.H. Taylor, D.J. Morgan, A.F. Carley, D.W. Knight, C.J. Kiely, G.J. Hutchings, ACS Nano **6**, 6600 (2012)
39. A. Santos, R.J. Lewis, G. Malta, A.G.R. Howe, D.J. Morgan, E. Hampton, P. Gaskin, G.J. Hutchings, Ind. Eng. Chem. Res. **58**, 12623 (2019)
40. S. Stoll, A. Schweiger, J. Magn. Reson. **178**, 42 (2006)
41. R. Underhill, R.J. Lewis, S.J. Freakley, M. Douthwaite, P.J. Miedziak, O. Akdim, J.K. Edwards, G.J. Hutchings, Technol. Rev. **62**, 417 (2018)
42. F. Li, Q. Shao, M. Hu, Y. Chen, X. Huang, ACS Catal. **8**, 3418 (2018)
43. S. Wang, K. Gao, W. Li, J. Zhang, Appl. Catal. A Gen. **531**, 89 (2017)
44. D.A. Crole, R. Underhill, J.K. Edwards, G. Shaw, S.J. Freakley, G.J. Hutchings, R.J. Lewis, Philos. Trans. R. Soc. A Math. Phys. Eng. Sci. **378**, 20200062 (2020)
45. C. Samanta, Appl. Catal. A Gen. **350**, 133 (2008)
46. C. Descamps, C. Coquelet, C. Bouallou, D. Richon, Thermochim. Acta **430**, 1 (2005)
47. Y. Kwon, K.J.P. Schouten, M.T.M. Koper, ChemCatChem **3**, 1176 (2011)
48. D.A. Bulushev, S. Beloshapkin, J.R.H. Ross, Catal. Today **154**, 7 (2010)
49. J.K. Edwards, A. Thomas, A.F. Carley, A.A. Herzing, C.J. Kiely, G.J. Hutchings, Green Chem. **10**, 388 (2008)
50. A. Georgi, M. Velasco Polo, K. Crincoli, K. Mackenzie, F.D. Kopinke, Environ. Sci. Technol. **50**, 5882 (2016)
51. J.J. Pignatello, E. Oliveros, A. MacKay, Crit. Rev. Environ. Sci. Technol. **36**, 1 (2006)
52. R.D. Armstrong, J. Hirayama, D.W. Knight, G.J. Hutchings, ACS Catal. **9**, 325 (2019)
53. A. Staykov, T. Kamachi, T. Ishihara, K. Yoshizawa, J. Phys. Chem. C **112**, 19501 (2008)
54. N.M. Wilson, D.W. Flaherty, J. Am. Chem. Soc. **138**, 574 (2016)
55. R.J. Lewis, G.J. Hutchings, ChemCatChem **11**, 298 (2019)

56. A.J.R. Hensley, Y. Hong, R. Zhang, H. Zhang, J. Sun, Y. Wang, J.S. McEwen, ACS Catal. **4**, 3381 (2014)
57. P.C. Su, H.S. Chen, T.Y. Chen, C.W. Liu, C.H. Lee, J.F. Lee, T.S. Chan, K.W. Wang, Int. J. Hydrogen Energy **38**, 4474 (2013)